WIND SETS FROM SMS IMAGES:

AN ASSESSMENT OF QUALITY FOR GATE

David Suchman

David W. Martin

Space Science and Engineering Center
University of Wisconsin
Madison, Wisconsin

October 1976

ABSTRACT

In this study we explore the accuracy, representativeness, and reproducibility of tracer winds in the area of the 1974 GARP Atlantic Tropical Experiment (GATE). These winds were generated by tracking clouds in Synchronous Meteorological Satellite (SMS) images displayed on the University of Wisconsin's Man-Computer Interactive Data Access System (McIDAS). Two questions are addressed: (1) How accurately can the cloud displacements be measured, and (2) To what extent do the cloud displacements represent the wind field?

Accuracy is evaluated in terms of data characteristics, McIDAS precision, and consistency. We find that for full resolution visible data neither navigation nor resolution errors significantly affect the tracking of clouds. An examination of consistency, defined as similarity of wind sets independently produced by several scientists tracking clouds from the same set of images, yields a RMS reproducibility of 2 $m \cdot s^{-1}$ for cirrus level and 1.3 $m \cdot s^{-1}$ for cumulus level winds. This is smaller than the "random" error generally attributed to cloud winds. In addition, the vorticity and divergence fields are qualitatively reproducible.

The discussion of representativeness centers about cloud height determination, and relating cloud motion to winds. Representativeness is examined through (1) the internal consistency of consecutive sets; (2) the consistency of the cloud wind field, including divergence and vorticity with such features as clusters, vortices, and clear areas; and (3) the difference between proximate satellite and ship winds. These differences were all under 3 $m \cdot s^{-1}$, which is close to the noise level of ship winds and better than radiosonde-radiosonde comparisons. We conclude that the

representativeness of cloud tracers to cumulus and cirrus level flow is good to within the accuracy of currently available ground truth data.

1. Introduction

A primary data requirement for extended weather forecasting is accurate wind measurements on a global scale. For the oceans, which until recently were scarcely monitored at all, this can only be achieved through special platforms such as buoys, carrier balloons and satellites.

Satellites offer several possibilities for inferring air motions; however, only one--cloud tracking--is used routinely. To get a cloud wind, successive positions of tracer clouds are measured in a sequence of satellite images. These positions are transformed into earth based coordinates of latitude and longitude. Velocity is calculated from changes in earth position.

Several systems now exist to measure cloud positions and generate tracer winds. At least one of these systems incorporates the hardware and software components needed to provide global winds on an operational basis. Yet there remain two major questions concerning the use of cloud displacement vectors as winds: (1) How accurately can the cloud displacements be measured? and (2) To what extent do the cloud displacements represent the wind field? These questions form the basis for this paper.

The answers to the question of accuracy appear in two forms. We begin with a brief description of the cloud tracking system developed at the University of Wisconsin, along with the problems inherent in tracking clouds, and their possible solutions. In addition, operator errors in obtaining the cloud displacements are examined in a series of reproducibility tests of wind sets.

The answers to the question of representativeness are less complete, and less direct. Hubert and Whitney (1971) found the "level of best fit" between satellite cloud tracer motions and nearby radar winds to be 200 mb

for cirrus level tracers and 850 mb for cumulus tracers. Differences at these levels of best fit were rather large: for speed, an average 9 knots low, 17 knots high; for direction an average of less than $\pm 40°$. In a study using ATS data, Fujita et al., (1975) concluded that the nature of low cloud motion should be better understood before cloud tracer motion can give an accurate representation of the low level wind field. Bengtsson and Morel (1974) in a GARP report concluded that the level of best fit for trade cumulus is closer to 950 mb; in addition, while expressing reasonable confidence on the accuracy of low level winds, the GARP Working Group on Numerical Experimentation (Bengtsson and Morel, 1974) questioned the utility of high level cloud winds mainly because of limitations in coverage.

In order to assess representativeness, direct comparisons of satellite winds with ground truth winds might seem most efficient in establishing satellite wind quality. However, it is rarely possible to achieve an adequate match in time, location, and altitude. This is true even of the GARP Atlantic Tropical Experiment (GATE), whose data are used as ground truth in the present study. Data availability limits comparisons to satellite winds with ship winds at the surface and at 250 mb. In addition, cloud winds typically are averaged over a one half to one hour period and are representative of motion within a 1 to 2 km layer; rawinsondes represent motion over a 1 to 2 min period within a 300 to 500 m layer. Given these limitations, the simplest comparison is visual--an overplot of ground based winds on the satellite wind field. Another possibility is quantitative comparisons of u and v components using objective analysis of satellite fields. Both comparisons appear in this paper.

Rawins are our ground truth, yet their accuracy also is open to question. Mosher and Sawyer (1975) compared against rawins the cloud tracer winds obtained during the 25 January-7 February 1975 Data Systems Test for the

First GARP Global Experiment (FGGE). Using about 1000 vectors obtained under operational conditions each day for 1800 GMT, they found that the mean of the absolute value difference between cloud and radar winds was about 5 $m \cdot s^{-1}$. The difference between adjacent radar winds (extrapolated downstream) was essentially the same--5 $m \cdot s^{-1}$. In a similar study using infrared data from 30-31 October 1974, Bauer (1976) compared cloud motions with soundings made coincidentally in time and space. He also found rawinsonde/rawinsonde, and cloud/rawinsonde differences to be the same--about 4.5 $m \cdot s^{-1}$. Bengtsson (1975) reports the random error of conventional upper-air synoptic soundings as ± 1 $m \cdot s^{-1}$ with total error ranging up to 10 $m \cdot s^{-1}$ in cases of strong winds.

Beyond direct comparisons of independently measured winds, the quality of satellite winds can be assessed through a careful comparison of the dynamics of a field with major features represented in the clouds. Examples include the association of persisting centers of low level convergence with active cloud clusters, divergence with cloud free regions, positive vorticity with cloud bands and vortices. Finally, we can capitalize on the inertia of the atmosphere to assess quality through the persistence of larger scale features within independently produced consecutive wind fields. Changes which do occur should be closely coupled to changes in the patterns and positions of clouds. Hence, the accuracy of cloud tracers as depictors of the wind field will be examined through direct comparisons, and through internal and physical consistency checks.

2. Cloud tracking system description

Wind sets are generated on the University of Wisconsin's Man-Computer Interactive Data Access System (McIDAS). This is an image storage, display, and processing system consisting of data archive, data access, video display, operator console, and computer control sections. [For complete details of

the McIDAS System see Suomi (1975), Smith (1975), and Chatters and Suomi (1975).] The essential difference between this and earlier systems is that measurements on McIDAS are referred to the original digital data. This is accomplished through electronic rather than photographic display of images. The key advantage of this scheme for wind determination follows from the use of the display only to choose a small image matrix out of the whole, thus preserving the excellent geometric fidelity of the spin scan camera (Chatters and Suomi, 1975).

Control of hardware and execution of the scientist's commands are achieved through a body of special software. With this system and associated software it is possible by simple key-ins to enhance an image, magnify it, combine adjacent images into loops of any length, vary loop speed by up to a factor of 30, navigate pictures, locate and track clouds in TV, image, or earth coordinates, and display the results as a vector plot superimposed on the original image. Two independent heads on the analog disk allow double looping of infrared and visible images, with instant single key transfer from one to the other, or interlacing of the two images. Cloud tracking may be done by either of two primary methods: cursor tracking of the cloud to the nearest TV line and element (pixel tracking), and image match tracking of the cloud to better than TV line-element resolution (correlation tracking).

Because of the small size of the tracer clouds and the general complexity of cloud patterns in the GATE area, most clouds have been tracked by the single pixel (picture element) method. The location of the cloud is determined by the position of a cursor, which is moved around the screen, by a position joy stick. Pixel tracking has been facilitated by the addition of a function called the velocity cursor, which enables the operator to compare and precisely match cursor motion to cloud motion.

Cloud top height is determined from both visible and infrared data using the method of Mosher (Suomi, 1975). Cloud emissivity is calculated from visible data. This emissivity is applied as a correction to the infrared black body temperature to obtain the cloud top temperature. Standard atmosphere soundings, corrected for latitude, yield a conversion of cloud top temperature to height. If visible data are absent, cloud height is computed using the uncorrected black body temperature. The cloud height function can either be requested independently of the wind calculation or it can be invoked as an automatic function as part of the cloud tracking subroutine. In the present case the trade cumulus and cirrus clouds sought as tracers ordinarily were sufficiently distinct to be easily recognized. A level for each type was assigned by the operator, and wind sets were generated one level at a time. The cloud height function helped in setting these levels, but its primary use was in checking the heights of clouds not immediately recognizable as trade cumulus (low) or cirrus (high).

3. Evaluation of cloud displacement measurements

Three principal sources of error in tracking clouds--navigation, image resolution, and the operator--were described by Hubert and Whitney (1971), and Bengtsson and Morel (1974). The significance of these errors is discussed below.

Navigation errors

A sequence of geosynchronous satellite pictures typically shows motion of the earth within the image frame. The primary causes of this motion are deviation from the ideal orbit and misalignment of the spin axes of the satellite and earth. Because it often is large compared to true cloud motion, earth motion must also be measured. Navigation is the means by which the

apparent motion of the earth is removed from the cloud motion computation. Through navigation, any pixel in the image coordinate system can be converted into earth coordinates of latitude and longitude. Residual navigation errors causing false motions will appear as systematic errors. Studies (see Smith, 1975) have shown that on McIDAS, absolute navigation errors can be held to one picture registration, usually are a small fraction of pixel size.

Resolution errors

The time and spatial resolution of the image impose the ultimate limits on the accuracy of the cloud tracked winds. If 30 min images have a pixel size of 2 n mi, the uncertainty in the position of an unchanging pixel sized cloud is (2 n mi)$\cdot$(30 min)$^{-1}$ = 4 n mi$\cdot$hr^{-1} or 2 m$\cdot$s^{-1}. Increasing the size of the cloud decreases the uncertainty of its position; however, larger clouds are less likely to be strictly passive tracers of the horizontal flow. On the other hand, the smaller clouds most likely to be passible tracers usually undergo the fastest changes, and the most rapid evolution. Selection of cloud tracers therefore involves compromises between size and lifetime and the match of cloud motion to ambient flow. Experience has shown that for tracking clouds in the tropics under typical conditions of cloud spacing, lifetime, and movement, a 30 min picture interval is well matched to 2 km (1 n mi) data; a 15 min interval to 1 km data. Therefore, relatively few vectors are lost if the nominal 30 min SMS visible data of GATE are displayed at a resolution reduced from the original by a factor of 2 or 3.

Operator errors

Prior to comparisons with ground truth, the consistency of our wind sets was examined. Consistency is a measure of the similarity of wind sets independently produced by several meteorologists tracking clouds from the same set of images. It is an assessment of the human element in cloud tracking. The sequence chosen for this reproducibility test was centered on 9 GMT,

5 Sept. 1974, when a rapidly developing cloud cluster was in the field of interest.

Cumulus (∿950 mb) and cirrus (∿250 mb) clouds were tracked by the single pixel method from visible and infrared pictures at 0830 GMT, 0900 GMT, and 0930 GMT. Wind sets for 0830-0900 GMT and 0900-0930 GMT were then averaged. Initially, six operators produced their own wind sets independently. These operators all had some experience in tracking winds.

The raw wind sets then underwent objective analysis [using a modified form of the WIND*SRI computer program (Mancuso and Endlich, 1973) with tight restrictions on extrapolations to data-free regions] to obtain grid point values of the u and v velocity components, and the fields of divergence and vorticity. These grid point values then were intercompared for u and v, divergence, and vorticity for each wind set. A total of ten randomly chosen intercomparison sets were made in overlapping valid data regions (approximately 75 grid points per case for velocity, and 40 grid points per case for divergence and vorticity).

The results of this initial reproducibility test for the four densest wind sets are shown in Table I. No one operator appeared to be significantly better than any other.

Two possible sources of error were noticed upon inspection of the qualitative features of the difference maps: (1) a few "bad" winds in a sparse data region often accounted for a large percentage of the mean difference between operators; and (2) some of the differences were caused by the nature of the objective analysis scheme.

To explore the reasons for wind discrepancies, the four densest wind sets were individually displayed on McIDAS as vectors superimposed on the images used for tracking. A group of meteorologists challenged questionable vectors. If the operator who generated the wind set could not justify these winds through reference to specific clouds at the appropriate levels,

TABLE I

ORIGINAL WIND REPRODUCIBILITY

(Four Nonedited Wind Sets)

	RMS Difference Between Operators	Mean Absolute Value
Low Level Winds		
$\bar{u}$	$1.07\ m \cdot s^{-1}$	$3.08\ m \cdot s^{-1}$
$\bar{v}$	$1.34\ m \cdot s^{-1}$	$5.06\ m \cdot s^{-1}$
Total Velocity	$1.71\ m \cdot s^{-1}$	$5.93\ m \cdot s^{-1}$
		Maximum Value
Vorticity	$18.92 \times 10^{-6}\ s^{-1}$	$40 \times 10^{-6}\ s^{-1}$
Divergence	$17.02 \times 10^{-6}\ s^{-1}$	$78 \times 10^{-6}\ s^{-1}$

	RMS Difference Between Operators	Mean Absolute Value
High Level Winds		
$\bar{u}$	$2.46\ m \cdot s^{-1}$	$8.29\ m \cdot s^{-1}$
$\bar{v}$	$1.62\ m \cdot s^{-1}$	$2.59\ m \cdot s^{-1}$
Total Velocity	$2.95\ m \cdot s^{-1}$	$8.69\ m \cdot s^{-1}$
		Maximum Value
Vorticity	$11.84 \times 10^{-6}\ s^{-1}$	$50 \times 10^{-6}\ s^{-1}$
Divergence	$24.46 \times 10^{-6}\ s^{-1}$	$86 \times 10^{-6}\ s^{-1}$

they were flagged. Deleting the flagged vectors yielded four reedited wind sets. (This reediting process has been applied to all subsequent GATE area wind sets.) Over the same period the objective analysis scheme was adjusted to give a better representation of the wind fields: smoothing was applied in regions of large shear to avoid anomalous values in the vorticity and divergence field; restrictions were added on data sparse regions to minimize the influence of one or two bad winds; more winds were used in the calculation of each grid point value.

Intercomparisons were repeated for the four reedited sets using the revised objective analysis scheme. These results are shown in Table II. For the gridpoint comparisons common to both Tables I and II, the increase in velocity reproducibility averaged 28%, vorticity, 32% and divergence, 33%. Hence, improvements in the editing and objective analysis significantly aided reproducibility.

A (RMS) reproducibility of 2 $m \cdot s^{-1}$ for the cirrus level, and 1.3 $m \cdot s^{-1}$ for the cumulus level was obtained. Considering the variability inherent in the differences in cloud-selection, the complexity of the case, and the inaccuracies of single-pixel tracking, this compares favorably with the ± 2 $m \cdot s^{-1}$ and ± 3 $m \cdot s^{-1}$ random error Bengtsson (1975) said was "characteristic" of low and high cloud derived winds. The better agreement found for the cumulus level clouds can be attributed to lower mean speeds, more tracers, and a more distinctive appearance of cumulus compared with cirrus.

The reproducibility of the vorticity and divergence fields are such that credence is established in their qualitative features, and to a reasonable degree, their quantitative aspects. This is particularly encouraging, inasmuch as both divergence and vorticity have proven to be highly difficult to measure with any degree of certainty by conventional methods.

TABLE II

REPRODUCIBILITY OF FOUR EDITED WIND SETS

Low Level Winds	RMS Difference Between Operators	Mean Absolute Value
$\bar{u}$	0.76 $m \cdot s^{-1}$	3.20 $m \cdot s^{-1}$
$\bar{v}$	1.04 $m \cdot s^{-1}$	5.25 $m \cdot s^{-1}$
Total Velocity	1.29 $m \cdot s^{-1}$	6.15 $m \cdot s^{-1}$
		Maximum Value
Vorticity	9.93×10^{-6} s^{-1}	34×10^{-6} s^{-1}
Divergence	11.62×10^{-6} s^{-1}	86×10^{-6} s^{-1}

High Level Winds	RMS Difference Between Operators	Mean Absolute Value
$\bar{u}$	1.71 $m \cdot s^{-1}$	8.56 $m \cdot s^{-1}$
$\bar{v}$	1.10 $m \cdot s^{-1}$	2.32 $m \cdot s^{-1}$
Total Velocity	2.03 $m \cdot s^{-1}$	8.87 $m \cdot s^{-1}$
		Maximum Value
Vorticity	9.93×10^{-6} s^{-1}	40×10^{-6} s^{-1}
Divergence	16.09×10^{-6} s^{-1}	77×10^{-6} s^{-1}

Hence, the question of cloud tracking accuracy has a partial answer. On a technical level tracking accuracy is consistent with the resolution limitations of the SMS data. On a human level there remains a relatively large margin of error arising from misinterpretation. This error can be much reduced through careful peer review and editing of the raw wind sets. The accuracy of wind sets so edited is such that their divergence and vorticity are basically the same.

4. Evaluation of wind accuracy

An evaluation of the representativeness of tracer winds to the true wind field is presented for three days--5, 10, and 18 September--typifying disturbed, suppressed, and moderately active conditions.

Completed wind sets are presented as maps of vectors. These vector plots include available ship winds when time and level differences are close enough to allow meaningful comparison. Except for a small group in the 18 September 1330 GMT set, all winds were generated by the single pixel method, using a velocity cursor. Tracking employed visible images; however, infrared images were available for height determination. In all cases at least five registered frames were available for viewing; tracking was done on the middle three frames at intervals of 15 to 30 minutes. Characteristics of individual sets are summarized in Table III. Visible and infrared picture pairs, one for each day, show the general distribution and organization of clouds.

The quality of the tracer winds are tested in three ways:
(a) comparison of satellite winds with GATE ship or aircraft winds having a reasonable time proximit , (b) internal consistency of consecutive sets, (c) comparison of satellite winds, derived vorticity and divergence fields with features such as clusters, vortices and squall lines.

Five September (day 248) was one of the most convectively active days of

TABLE III

CHARACTERISTICS OF GATE WIND SETS

Day	Sequence	Image Interval (min)	Visible Image Resolution (km)	Load Center (lat)	(long)
5 Sept.	0830, 0900, 0930 GMT	30	2	0830 N	2330 W
	1200, 1230, 1300 GMT	30	2	0830 N	2330 W
	1430, 1500, 1530 GMT	30	2	0830 N	2330 W
10 Sept.	1215, 1230, 1245 GMT	15	1	1214 N	2314 W
	1215, 1230, 1245 GMT	15	1	0830 N	2330 W
	1215, 1230, 1245 GMT	15	1	0450 N	2335 W
	1445, 1500, 1515 GMT	15	2	0830 N	2330 W
18 Sept.	1315, 1330, 1345 GMT	15	1	0925 N	2130 W
	1445, 1500, 1515 GMT	15	1	0925 N	2130 W

GATE. A large, well-organized cluster (see Fig. 1) dominated the center of the ship array much of the day. Two distinct centers of activity were associated with this cluster: one to the east that reached maturity early in the day and the one to the west that developed in the morning and began decaying by early afternoon. At low levels, the strong flow into the clusters in early morning (mainly from the northeast and southwest) gradually diminished as the day progressed, with the strongest inflow being in the western parts late in the afternoon. The high level flow, initially from southeast to northwest over the northern region and northeast to southwest over the southern region, became dominated by the strong outflow from the two convective centers as the day progressed.

Figures 2 a-c and 3 a-c show the McIDAS derived cumulus and cirrus level cloud tracers centered on 0900 GMT, 1230 GMT, and 1500 GMT. At the time that these and the other wind sets presented in this paper were produced, satellite images were the sole source of information on winds and flow patterns in the areas of interest. Ship sonde winds taken from GATE synoptic-scale surface and 250 mb maps at 12 GMT compose the ground truth which is the basis for these comparisons. These sonde winds and derived streamlines (Dean, 1976) are plotted on Figs. 2b and 3b.

The correspondences for low and high level winds in regions of both satellite and sonde observations are excellent (Figs. 2b, 3b). Rather surprisingly, cloud winds are a far better match to surface then to 850 mb winds. The tendency for ship winds to exceed satellite winds in the southwestern part of the area at upper levels (Fig. 3b) may be the result of lower, layered cirrus associated with a small developing convective cell near 6°N, 27°W.

When the 12 GMT sonde observations (given to the nearest five knots)

were compared with the closest objectively analyzed grid point wind derived from the 1230 GMT wind set, the average absolute difference in speed was 1.9 $m \cdot s^{-1}$ for the cumulus level, and 2.9 $m \cdot s^{-1}$ for the cirrus level. The absolute differences in direction for both cases averaged about 20°. This is certainly well within the limits of accuracy for the sonde observations, and other conventional systems as described by Bengtsson (1975). They are also less than half the deviations found by Hubert and Whitney. Differences were randomly distributed for the low level; at the cirrus level tracer wind were consistently slower, probably because of cirrus evaporation along the downstream edge.

Figs. 4a and 4b show an example of the objectively analyzed grid point winds (as derived from the 1230 GMT cloud tracer field). At the cumulus level, two centers of convergence can be identified, corresponding to the two centers of convection: one at about 9°N, 20°30'W, and the other at 9°N, 25°30'W. At the cirrus level, strong divergence corresponds to both the mature eastern convective center, as well as for the developing western center.

The corresponding low and high level divergence fields (derived from the grid-point winds) appear on Figs. 5a and 5b. The strong low level convergence into the developing western cluster, and the pronounced upper level divergence associated with both clusters are very clearly shown--both the qualitative and quantitative features are very reasonable. Hence, for this very active system, the cloud tracer winds depict the "true" wind field very accurately by exhibiting internal consistency of consecutive sets, good correspondence of wind and divergence fields with major cloud features, plus good agreement between cloud and sonde winds.

Ten September (day 253) was at the opposite end of the weather spectrum. There was little organized convection and few clouds (Fig. 6). Cumulus level tracers show an elongated anticyclonic gyre at 5° and 6°N (Fig. 7a, 7b). Winds in the clear area north of the gyre axis were light westerly, with a weak maximum in west northwest flow. These features appear also in the surface ship winds. The largest discrepancies occur in the weak wind area close to the center of the gyre.

Flow at the cirrus level was generally westward with difluence in the southeast over and around a mature cloud cluster between 5°N and 7°N. Ship winds very closely match satellite winds in speed; however, through the center section between 7°N and 8°N, ship wind directions are more northerly, by as much as 30 degrees close to the cluster at 7°N.

Eighteen September (day 261) was neither as suppressed as 10 September nor as active as 5 September. Clouds at the trade cumulus level were abundant. In the central and northwestern parts of the analysis area these cumuli swelled to congesti and cumulonimbi, forming two small, rather disorganized clusters (Fig. 8). The maps of low cloud tracers show that these clusters developed in an anticyclonic south to southwesterly current (Fig. 9a, 9b). Within this current there was a slight direction convergence, and a fairly marked speed convergence, both in the vicinity of the central cluster (at 9°21'N, 21°00'W).

Ship winds and satellite winds agree to within 10 degrees, except at the Vanguard (10°N, 23°20'W), where the direction difference is about 50°. Speeds also are very close.

Cirrus clouds were not as uniformly distributed; nevertheless, the large scale pattern is well defined (Fig. 10a, 10b). Flow at the cirrus

level turned anticyclonically from east to southeast. There was a slight downstream decrease in speed, with a difluent pattern west and southwest of center, and over the central cluster at 15 GMT.

Although no ship winds lie close to the satellite winds, the patterns formed by each set are mutually consistent. Principal features of the satellite field--including anticyclonic flow, difluence, and downstream deceleration--appear in the ship winds as well.

Comparisons of the 12 GMT soundings with the nearest objectively analyzed grid point winds for 1330 GMT show close agreement: differences in speed were 1.0 $m \cdot s^{-1}$ for low and 2.7 $m \cdot s^{-1}$ for high level winds, while the directional differences were 25° and 16°, respectively. None of the deviations were systematic. These correspondences were somewhat better than those of 5 September partly due to the higher resolution of the data, and partly due to the relative simplicity of the flow patterns.

5. Conclusions

Using a variety of tests and comparisons for meso-synoptic scale wind sets covering flow patterns from the simple to the complex, we have examined McIDAS derived cloud tracer winds. Our evaluation is based on the accuracy of the measurement of cloud displacements and the representativeness of cloud winds to the "true" wind field. Findings on both these points are positive.

In every case examined, not only were the dominant features defined by conventional measurements contained in the fields of satellite winds, the satellite wind fields were denser and in general contained more detail than the sonde winds. Differences between proximate satellite and ship winds were all under 3 $m \cdot s^{-1}$, which is close to the noise levels in the ship winds and error levels inherent in making comparisons of such disparate measurements.

The wind fields for 5 September are entirely consistent with the major cloud features, and the qualitative features of the divergence and vorticity fields are realistic.

Though the development of techniques for obtaining cloud tracer winds is far from complete, we conclude that if tropical cumulus and cirrus clouds are tracked with sufficient care by experienced operators, the wind fields obtained by present methods are at least on a par, in terms of point accuracies, with winds derived by conventional means. Because the weakest link now is assigning the right height to each cloud that is tracked, the principal limitation of these winds in meeting needs for global winds is likely to be vertical coverage rather than tracking accuracy. This problem is made more acute by large biases in the vertical distribution of tropical clouds. For the immediate needs of GATE, trade cumulus and cirrus cloud winds can contribute significantly to closing the observational gaps that developed in the large (A) scale sounding network over the Atlantic. More important, perhaps, is the contribution they can make to defining the dynamic structure and environment of the cloud ensembles that are the focus of GATE. This work serves a second purpose, the improvement of satellite winds through independent observations of clouds and wind.

ACKNOWLEDGEMENTS

Thanks are extended to Brian Auvine, Gary Chatters, John Stout, and Don Wylie, who contributed as cloud trackers. Gary Chatters served as navigator and as advisor on all aspects of McIDAS operation. Anthony Schreiner and Walter Knaack assisted in data reduction and analysis, Dana Wooldridge in drafting figures. Barbara Mueller typed the manuscript, which was reviewed by Verner Suomi.

Recognition is also due those who gave us McIDAS and keep it going: the lamplighters--Verner Suomi and Thomas Haig; the builders--Terry Schwalenberg, John Benson, Eric Smith, J. T. Young, Mahendra Shah, Fred Mosher, Dennis Phillips, and Ralph Dedecker; the keepers--Eric Suomi, Gary Chatters, and Michael Becker.

This work was supported under NASA Contracts NAS5-21798 and NAS5-23296, Verner Suomi, Principal Investigator.

REFERENCES

Bauer, K. E., 1976: A Comparison of Cloud Motion Winds With Coinciding Radiosonde Winds. Mon. Wea. Rev., 104, 922-931.

Bengtsson, L., 1975: Four-Dimensional Assimilation of Meteorological Observations. GARP Publications Series No. 15, World Meteorological Organization.

_____ and P. Morel, 1974: The Performance of Space Observing Systems for the First GARP Global Experiment. The GARP Working Group on Numerical Experimentation, World Meteorological Organization.

Chatters, G. C. and V. E. Suomi, 1975: The Applications of McIDAS. IEEE Transactions on Geoscience Electronics, GE-13, 137-146.

Dean, G., 1976: personal communication, Florida State University.

Fujita, T. T., E. W. Pearl, and W. E. Shenk, 1975: Satellite-Tracked Cumulus Velocities. J. Appl. Meteor., 14, 407-413.

Hubert, L. F. and L. F. Whitney, jr., 1971: Wind Estimation from Geostationary-Satellite Pictures. Mon. Wea. Rev., 99, 665-672.

Mancuso, R. L. and R. M. Endlich, 1973: User's Manual, Wind Editing and Analysis Program: Spherical Grid. (WEAP-1A), Stanford Research Institute.

Mosher, F. R. and B. Sawyer, 1975: Comparison of Wind Measurement Systems: Cloud Tracked Winds vs. Rawinsonde Winds and Rawinsonde Winds vs. Rawinsonde Winds. In Preliminary Assessment of the Cloud Tracking System Developed at the University of Wisconsin, SSEC, Univ. of Wisconsin.

Smith, E. A., 1975: The McIDAS System. IEEE Transactions on Geoscience Electronics, GE-13, 123-136.

Suomi, V. E., Principal Investigator, 1975: Man-Computer Interactive Data Access System (McIDAS), Final Report Contract NAS5-23296, Univ. of Wisconsin, Madison.

FIGURE LEGENDS

Figure 1a SMS-1 images for 1230 GMT, 5 September 1974, photographed from McIDAS display. Cursor is centered on the B-Array, at 8°30'N, 23°30'W; length of sides ∿60 km, visible channel, resolution reduced by a factor of two.

Figure 1b Same as Fig. 1a, except infrared channel enlarged four times to scale of visible image.

Figure 2a Cumulus level cloud tracer motions, 0900 GMT, 5 September 1974.

Figure 2b Cumulus level cloud tracer motions, 1230 GMT, 5 September 1974; surface ship winds and streamline analysis superimposed, 1200 GMT [Dean, 1976].

Figure 2c Same as Fig. 2a, except 1500 GMT.

Figure 3a Cirrus level cloud tracer motions, 0900 GMT, 5 September 1974.

Figure 3b Cirrus level cloud tracer motions, 1230 GMT, 5 September 1974; 250 mb ship winds and stremaline analysis superimposed, 1200 GMT [Dean, 1976].

Figure 3c Same as Fig. 3a, except 1500 GMT.

Figure 4a Objectively analyzed cumulus level grid point winds, 1230 GMT, 5 September 1974.

Figure 4b Same as Fig. 4a, except cirrus level.

Figure 5a Cumulus level divergence (10^{-6} s^{-1}), 1230 GMT, 5 September 1974.

Figure 5b Same as Fig. 5a, except cirrus level.

Figure 6a SMS-1 images for 1230 GMT, 10 September 1974. Cursor is centered in the B-Array, at 8°30'N, 23°30'W; length of sides ∿30 km, visible channel, full resolution.

Figure 6b Same as Fig. 6a, except infrared channel enlarged eight times to scale of visible image.

Figure 7a Cumulus level cloud tracer motions, 1230 GMT, 10 September 1974; surface ship winds, 1200 GMT.

Figure 7b Same as Fig. 7a, except cirrus level.

Figure 8 SMS-1 images of 1330 GMT, 18 September 1974. Cursor located at 9°25'N, 21°30'W; diameter ∿30 km, visible channel, full resolution.

Figure 8b Same as Fig. 8a except infrared channel enlarged eight times to scale of visible channel.

Figure 9a Cumulus level cloud tracer motions (light arrows), 1330 GMT, 18 September 1974; surface ship winds (heavy arrows with circles), 1200 GMT.

Figure 9b Cumulus level cloud tracer motions, 1500 GMT, 18 September 1974.

Figure 10a Cirrus level cloud tracer motions (light arrows), 1330 GMT, 18 September 1974.

Figure 10b Cirrus level cloud tracer motions, 1500 GMT, 18 September 1974.

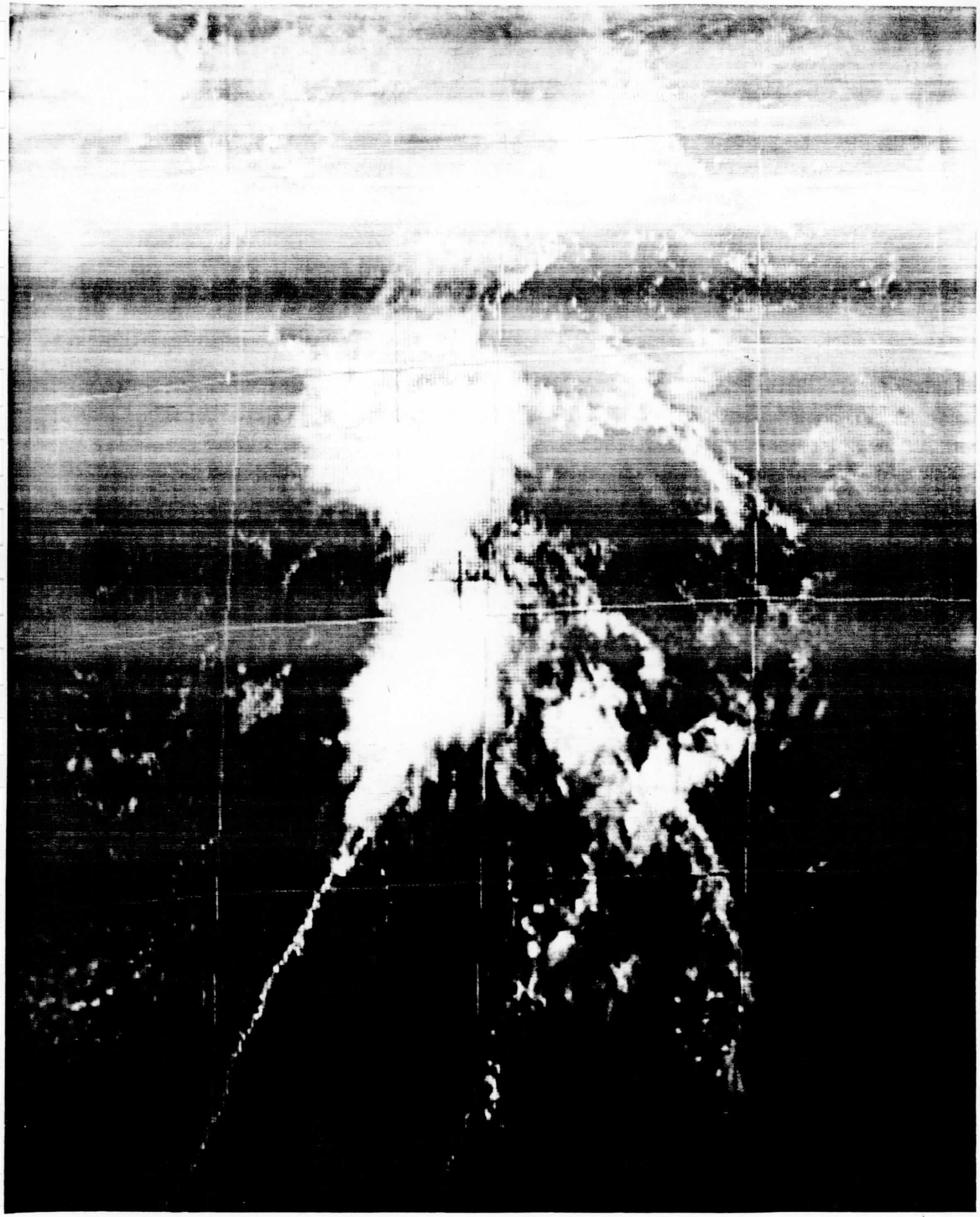

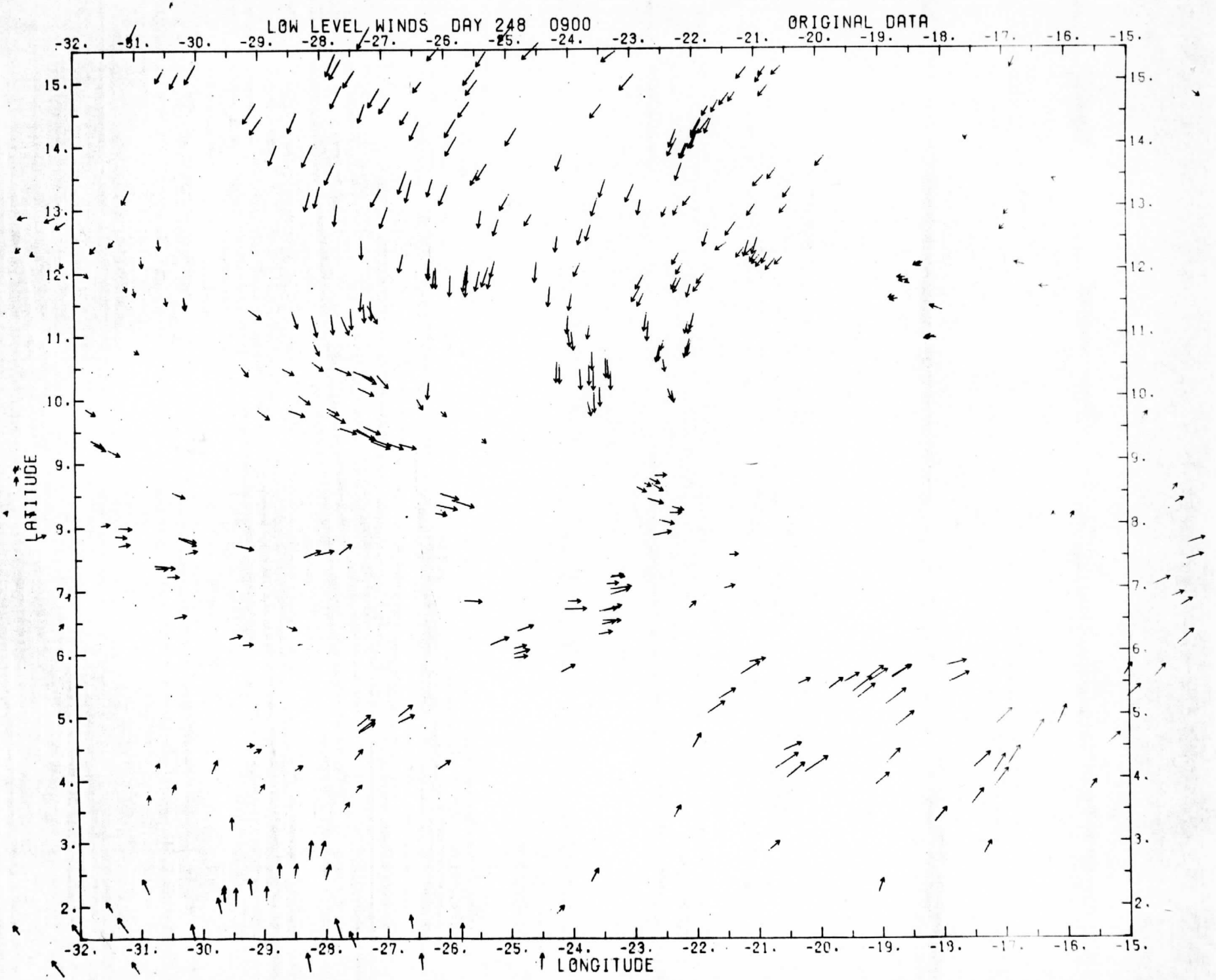
LOW LEVEL WINDS DAY 248 0900
ORIGINAL DATA
-32. -31. -30. -29. -28. -27. -26. -25. -24. -23. -22. -21. -20. -19. -18. -17. -16. -15.
15. 14. 13. 12. 11. 10. 9. 8. 7. 6. 5. 4. 3. 2.
LATITUDE
LONGITUDE

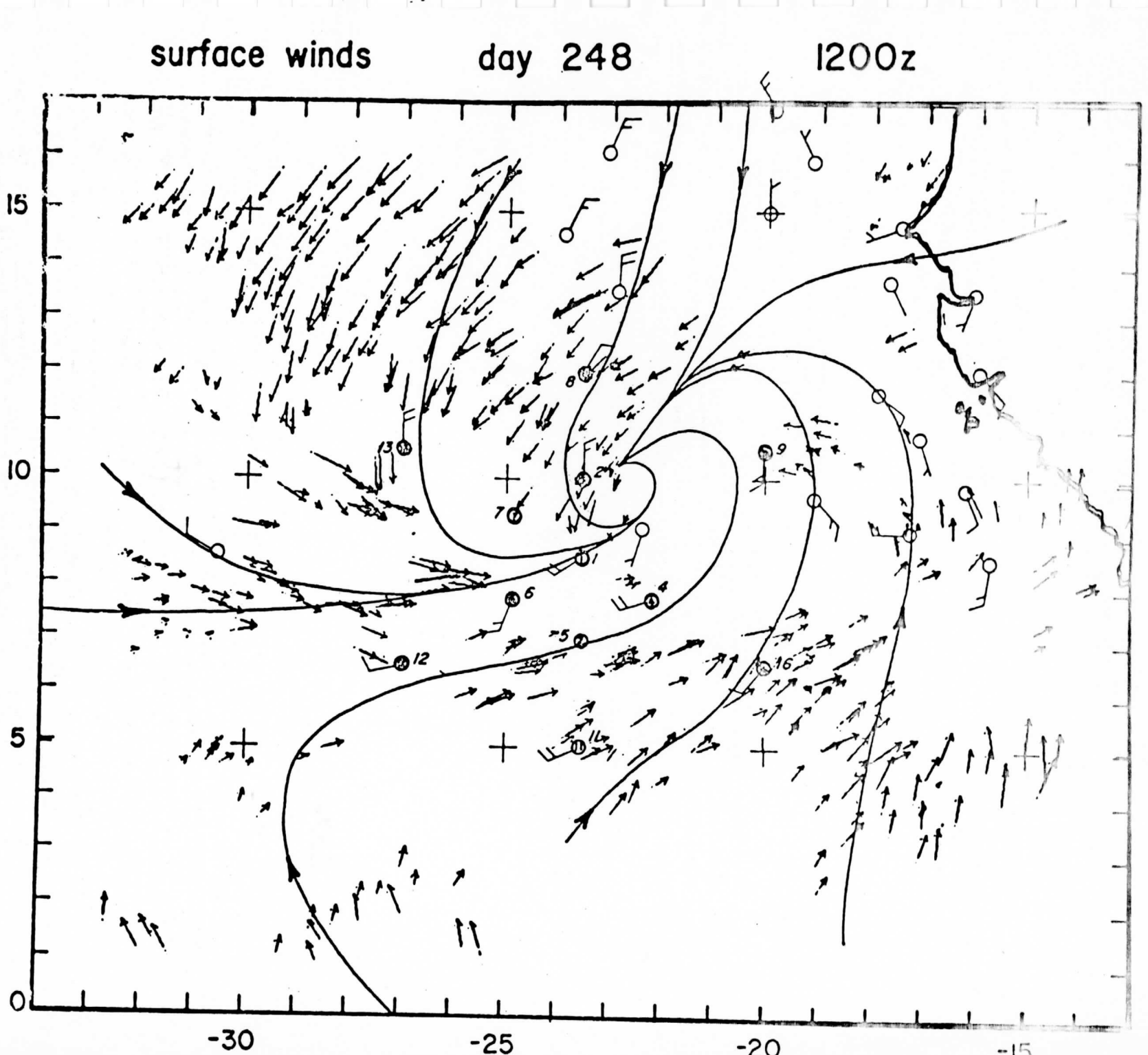
surface winds
day 248
1200z
15
10
5
0
-30
-25
-20
-15

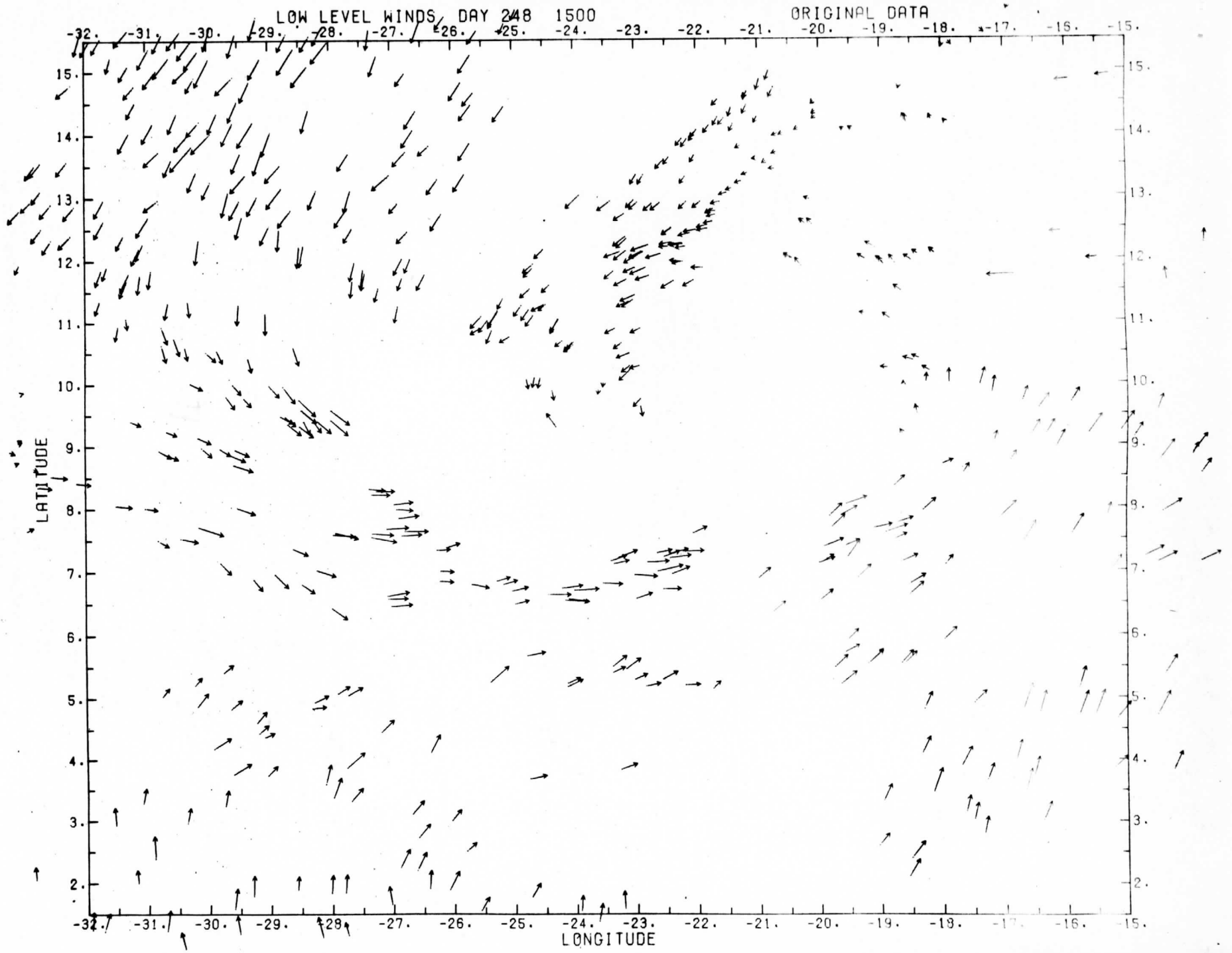
LOW LEVEL WINDS, DAY 248 1500
ORIGINAL DATA
-32. -31. -30. -29. -28. -27. -26. -25. -24. -23. -22. -21. -20. -19. -18. -17. -16. -15.
15. 14. 13. 12. 11. 10. 9. 8. 7. 6. 5. 4. 3. 2.
LATITUDE
LONGITUDE

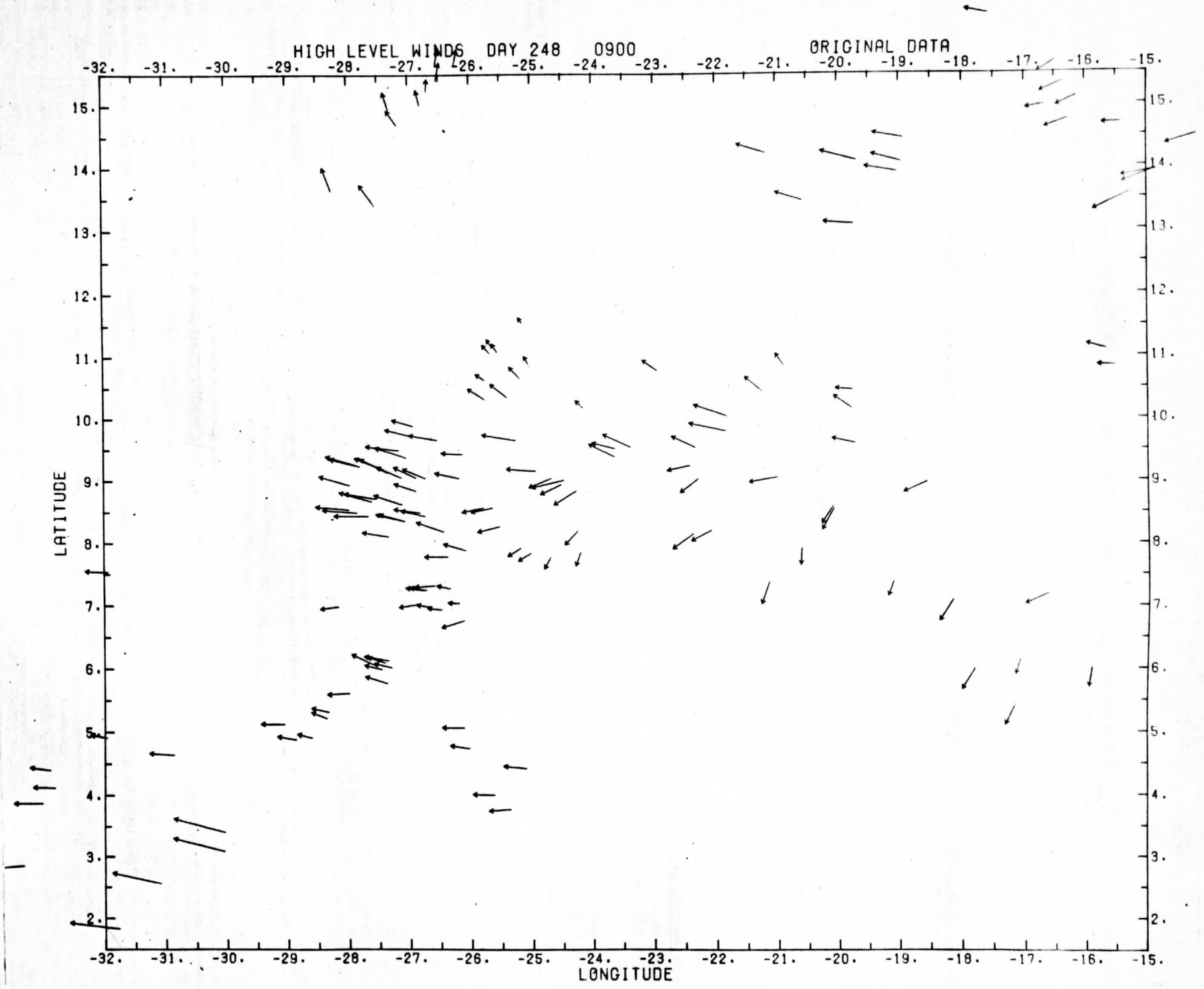
HIGH LEVEL WINDS DAY 248 0900
ORIGINAL DATA
LATITUDE
LONGITUDE
-32. -31. -30. -29. -28. -27. -26. -25. -24. -23. -22. -21. -20. -19. -18. -17. -16. -15.
15. 14. 13. 12. 11. 10. 9. 8. 7. 6. 5. 4. 3. 2.

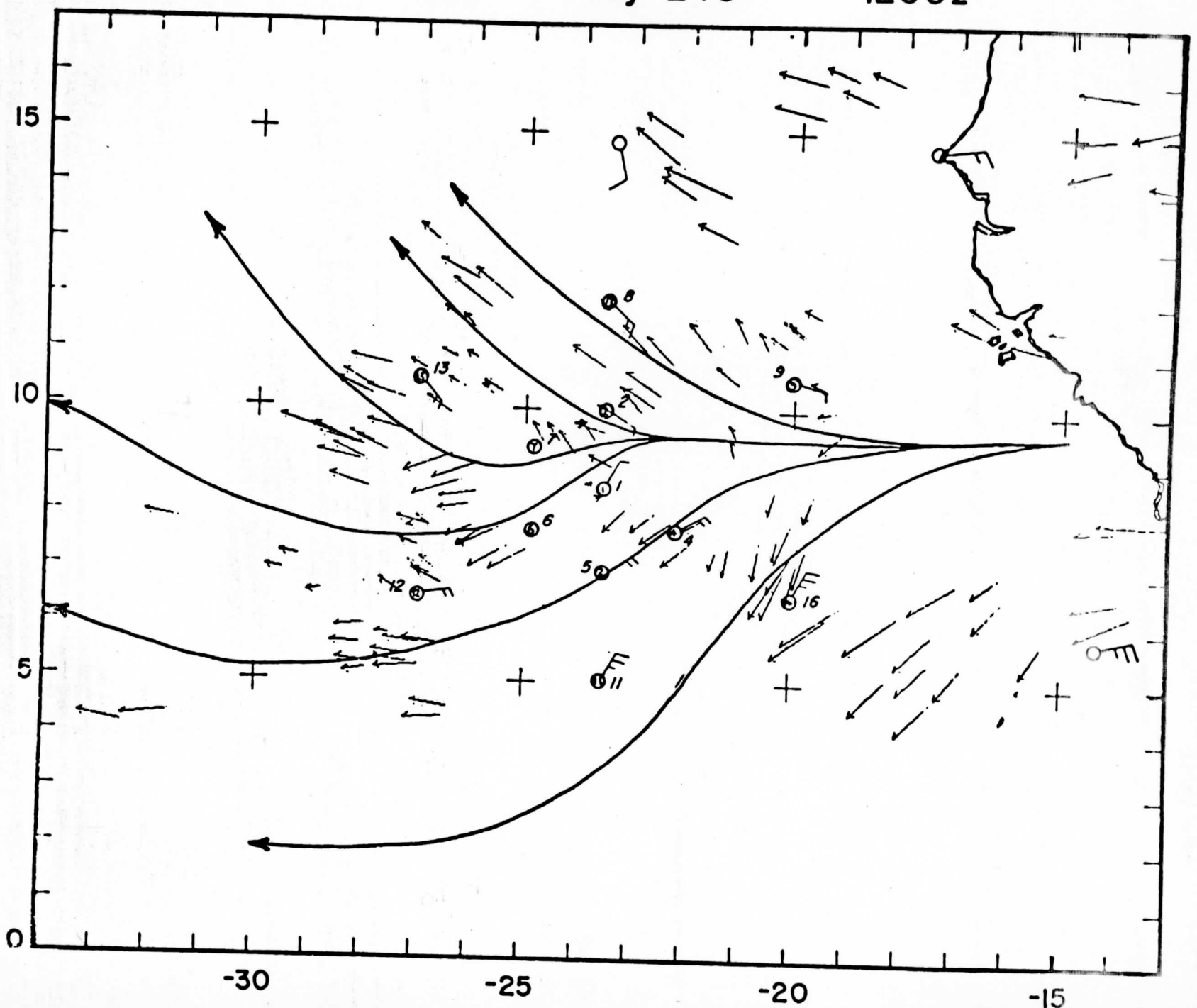
250 mb winds
day 248
1200z
15
10
5
0
-30
-25
-20
-15

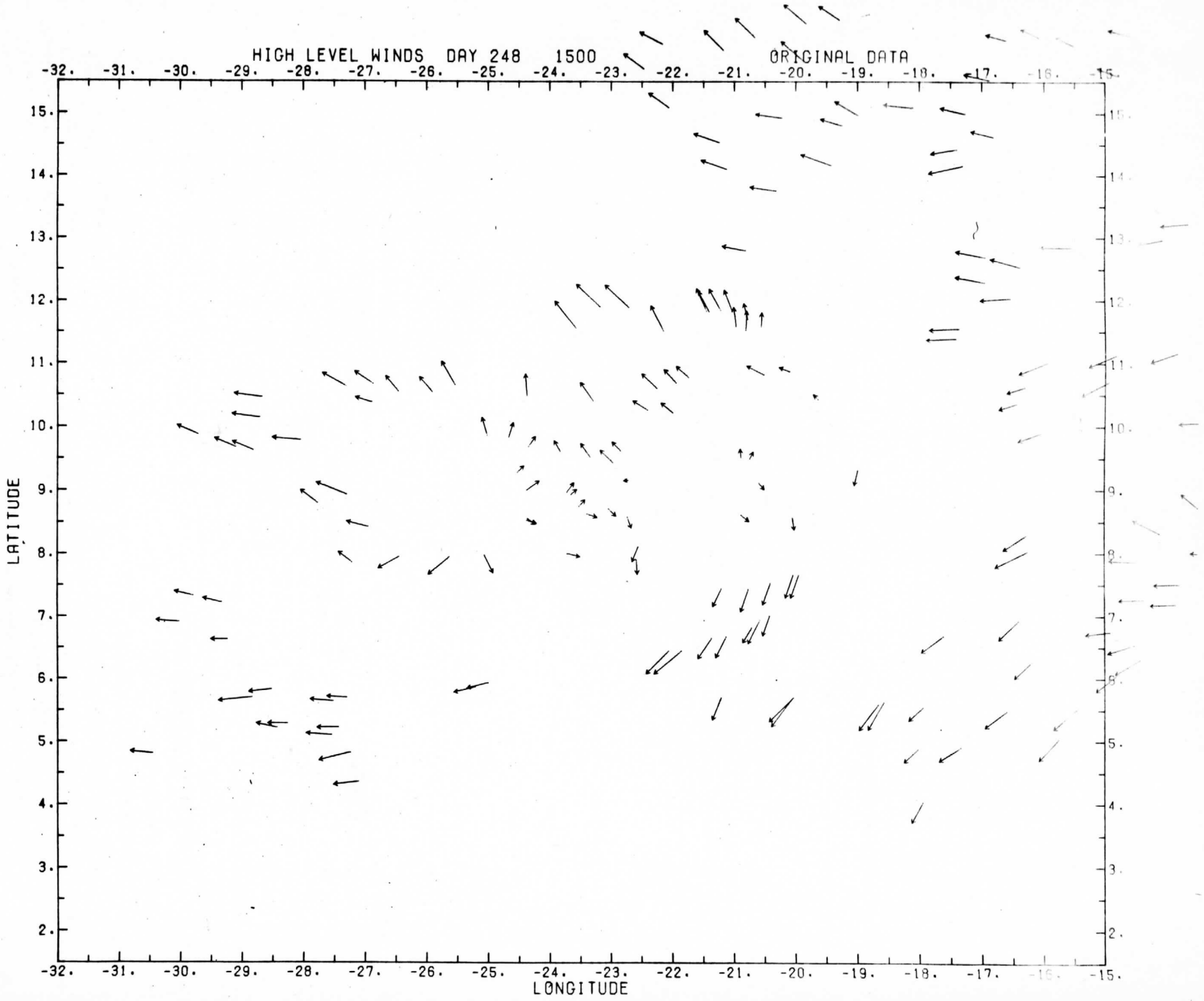
HIGH LEVEL WINDS DAY 248 1500 ORIGINAL DATA
-32. -31. -30. -29. -28. -27. -26. -25. -24. -23. -22. -21. -20. -19. -18. -17. -16. -15.
15. 14. 13. 12. 11. 10. 9. 8. 7. 6. 5. 4. 3. 2.
LATITUDE
LONGITUDE

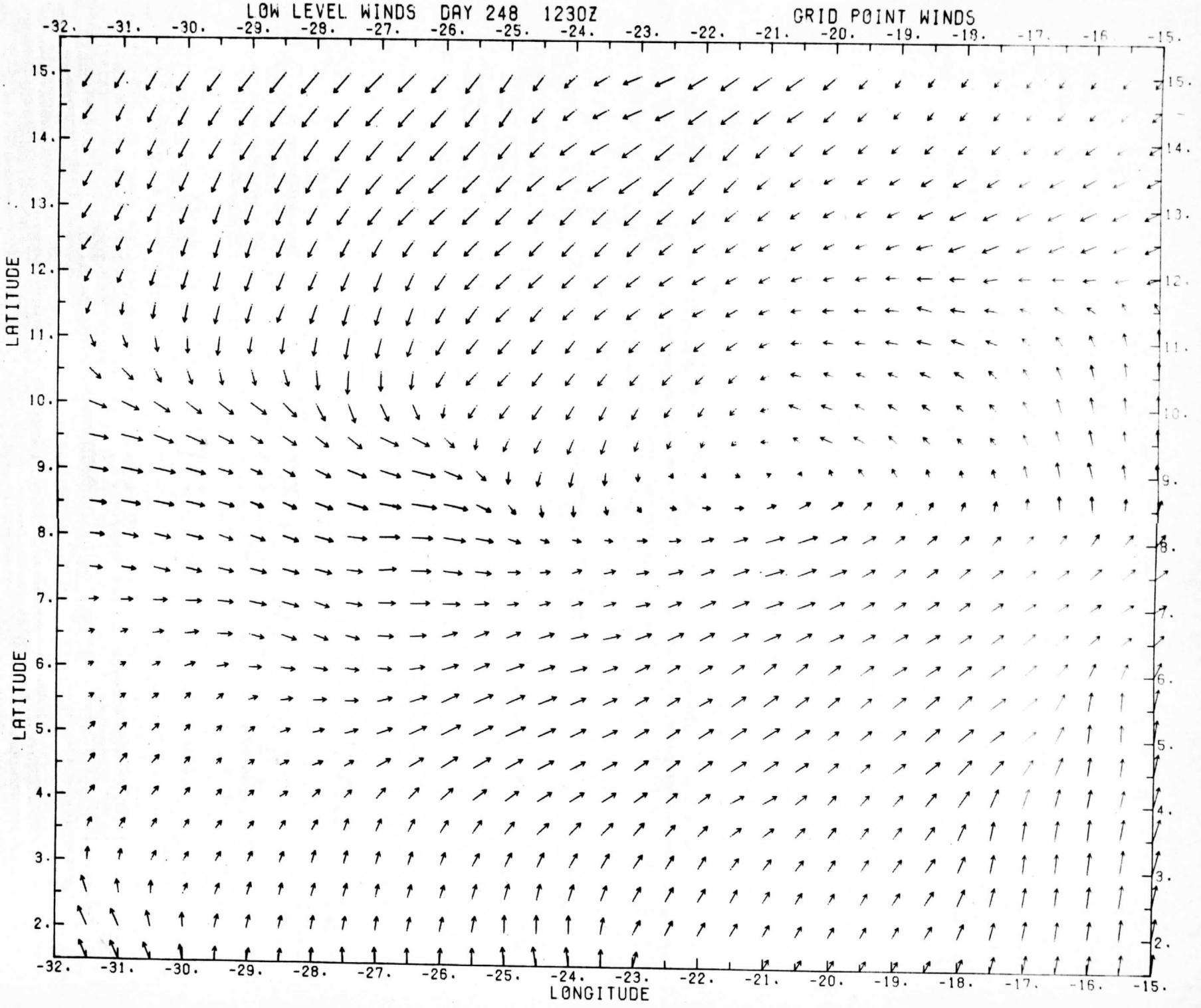
LOW LEVEL WINDS DAY 248 1230Z
GRID POINT WINDS
LATITUDE
LONGITUDE
-32. -31. -30. -29. -28. -27. -26. -25. -24. -23. -22. -21. -20. -19. -18. -17. -16. -15.
15. 14. 13. 12. 11. 10. 9. 8. 7. 6. 5. 4. 3. 2.

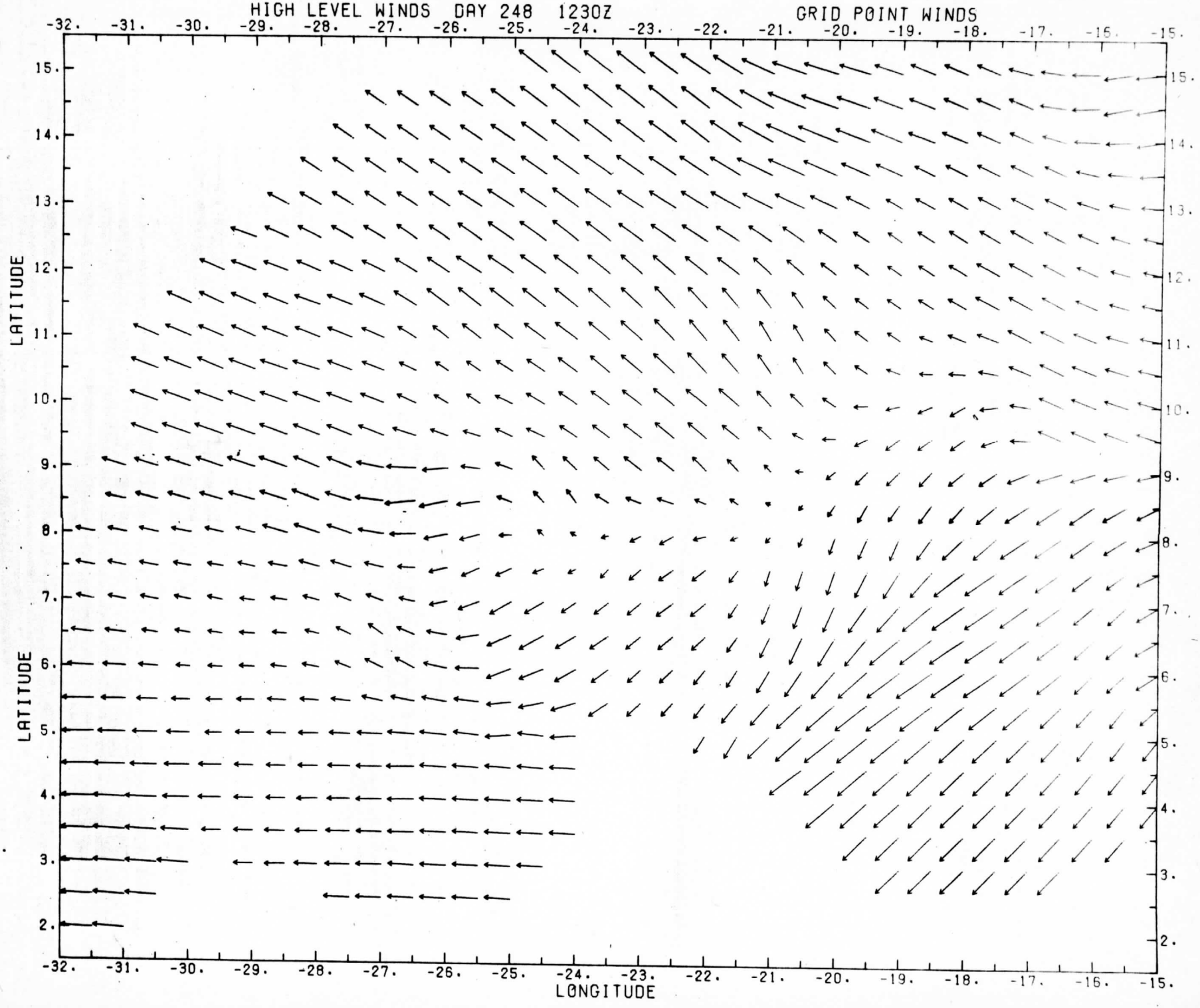
HIGH LEVEL WINDS DAY 248 1230Z
GRID POINT WINDS
-32. -31. -30. -29. -28. -27. -26. -25. -24. -23. -22. -21. -20. -19. -18. -17. -16. -15.
15. 14. 13. 12. 11. 10. 9. 8. 7. 6. 5. 4. 3. 2.
LATITUDE
LONGITUDE

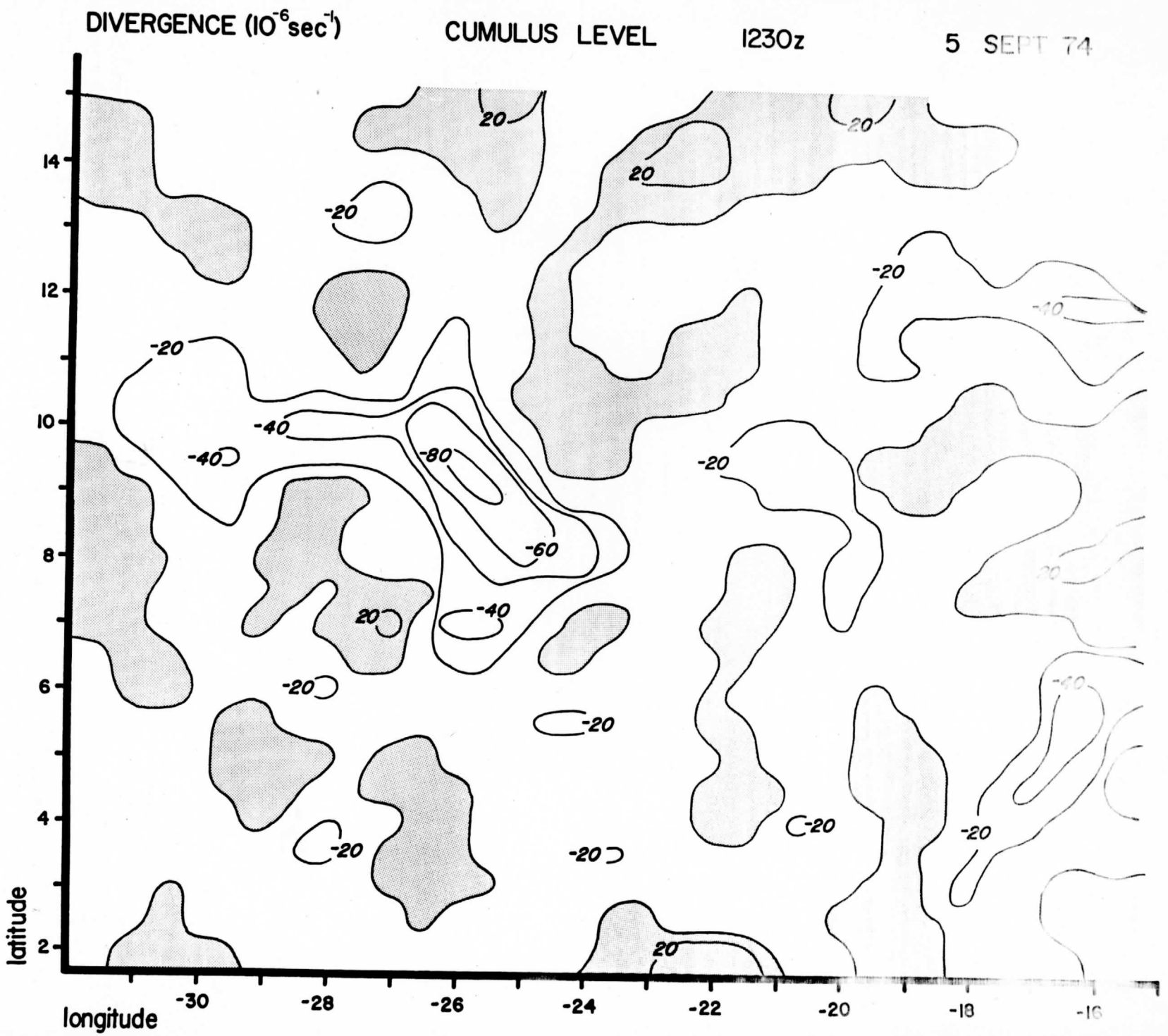
DIVERGENCE (10^{-6}sec^{-1})
CUMULUS LEVEL
1230z
5 SEPT 74
latitude
longitude
14
12
10
8
6
4
2
-30
-28
-26
-24
-22
-20
-18
-16
20
-20
-40
-80
-60
-10

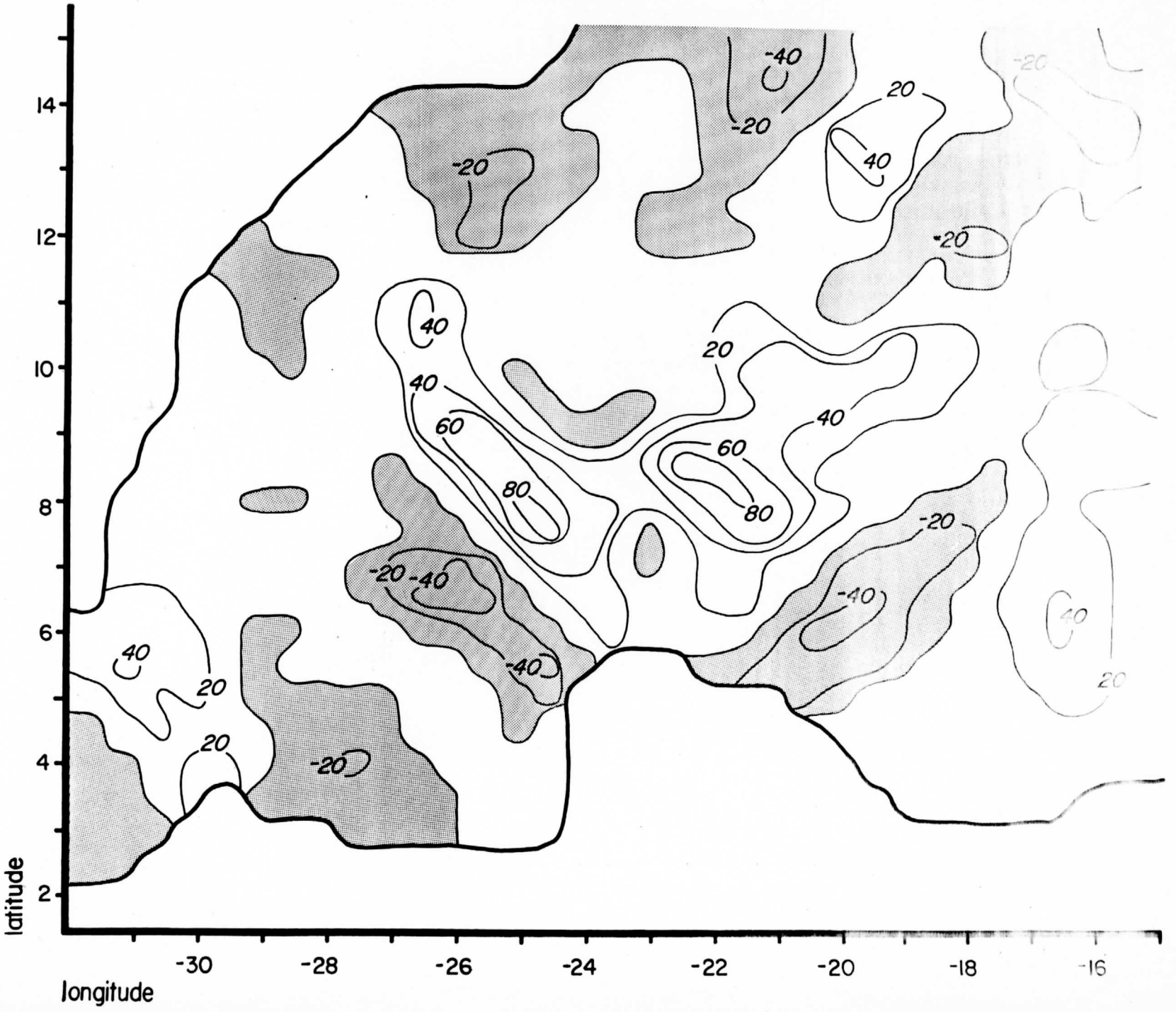
DIVERGENCE (10^{-6} sec^{-1})
CIRRUS LEVEL
1230z
5 SEPT
-40
-20
20
40
-20
-20
40
-20
40
40
60
20
40
60
80
80
-20
-20
-40
-40
-20
-40
40
20
20
-20
40
20
14
12
10
8
6
4
2
latitude
-30
-28
-26
-24
-22
-20
-18
-16
longitude

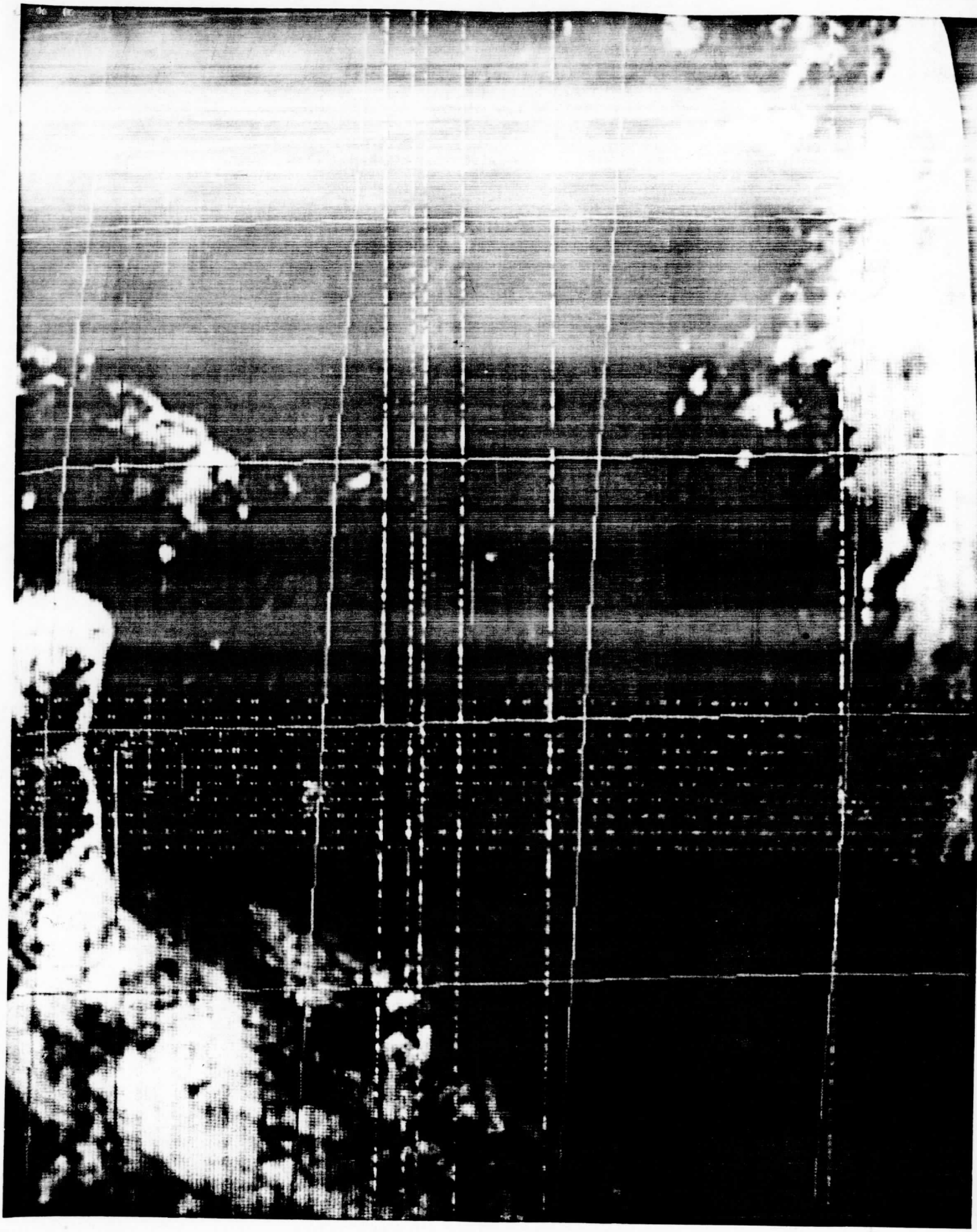

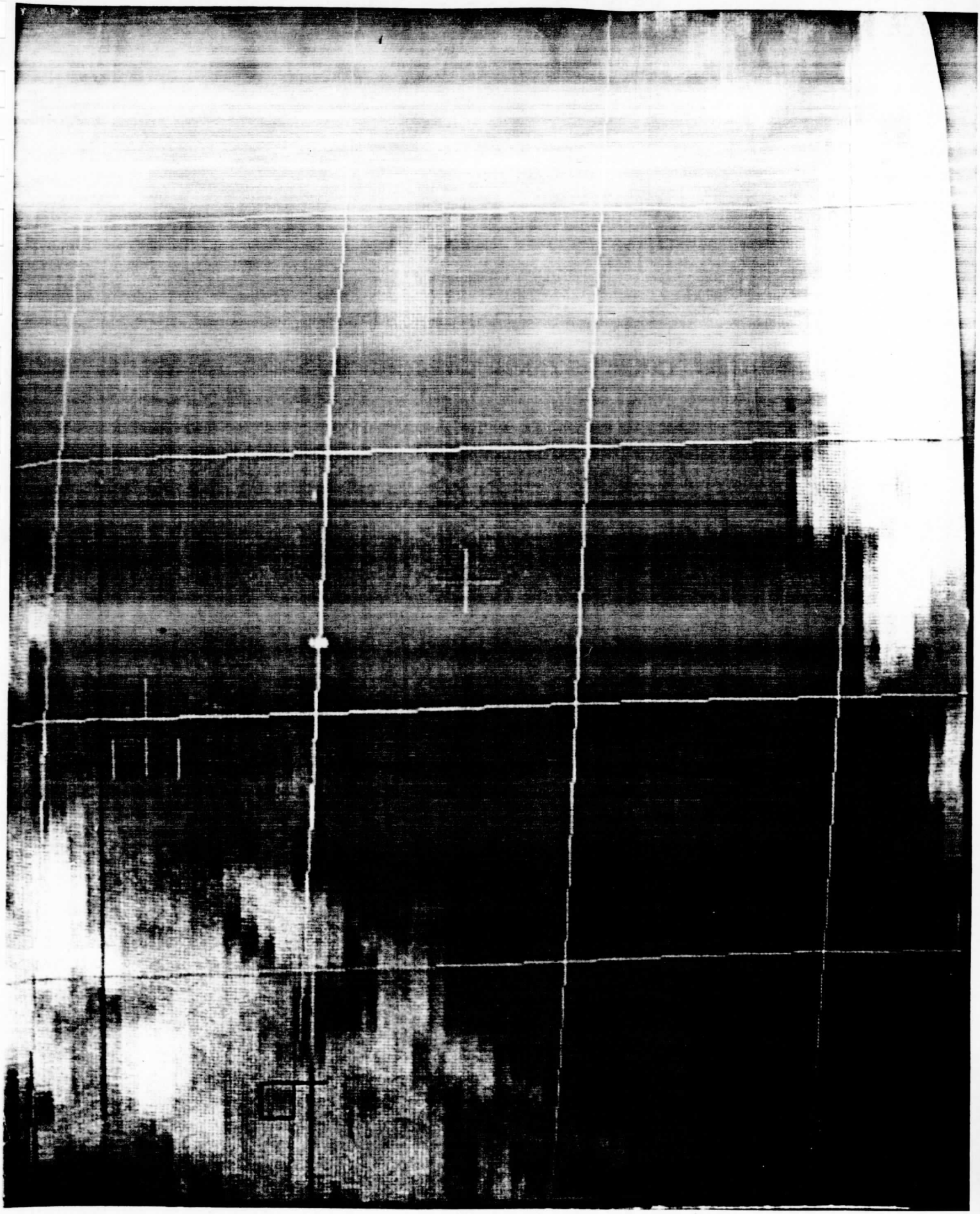

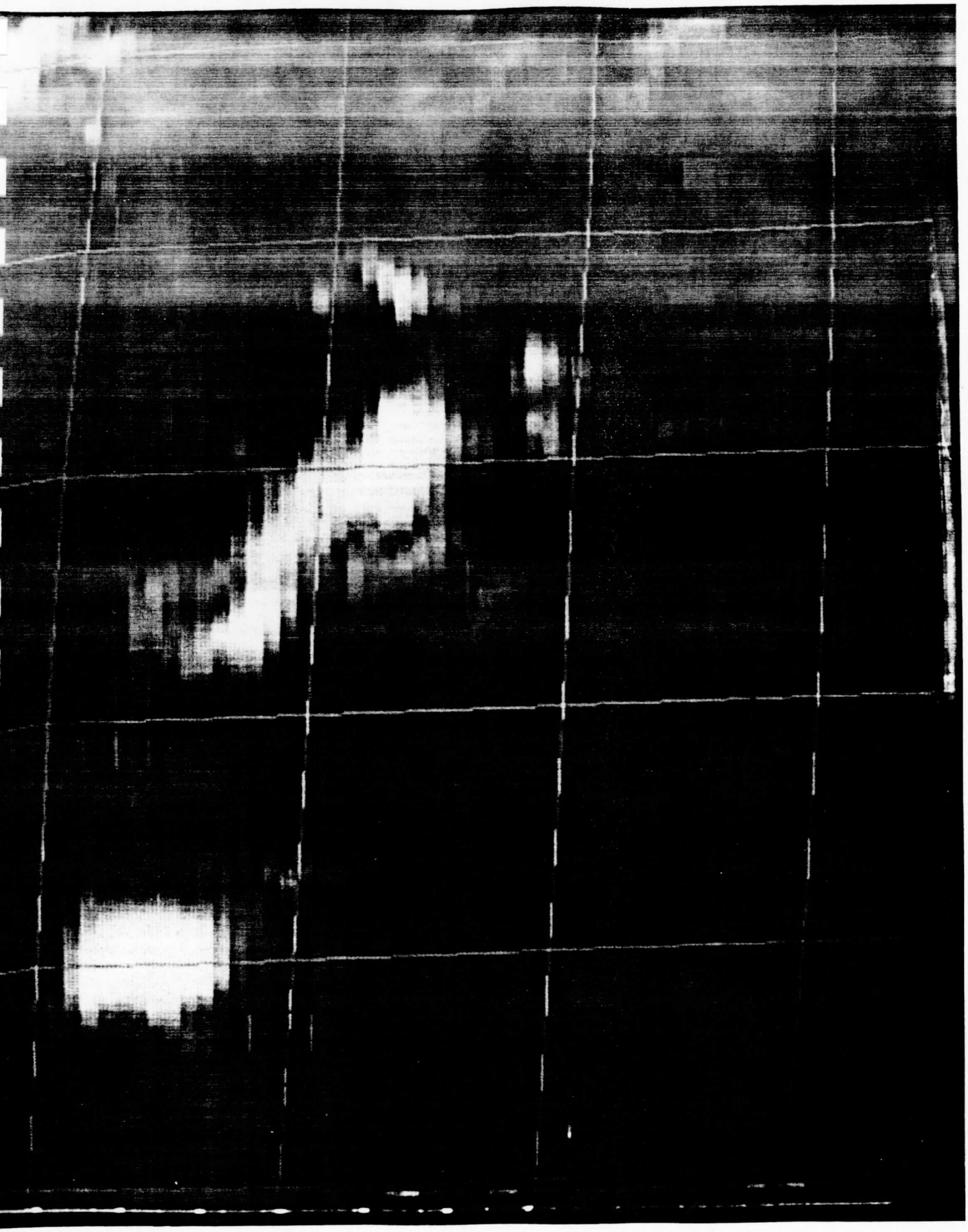

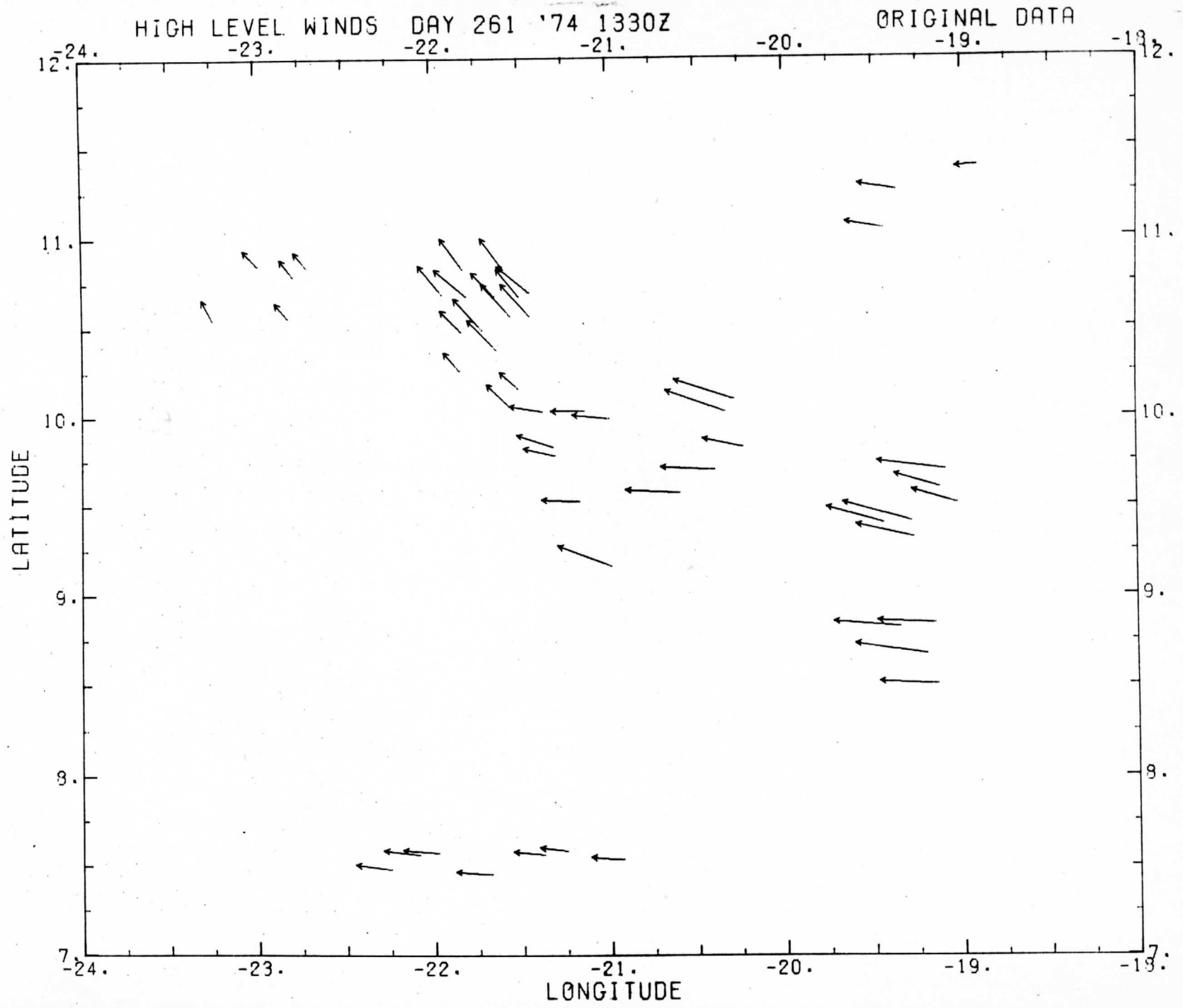
HIGH LEVEL WINDS DAY 261 '74 1330Z
ORIGINAL DATA
-24.
-23.
-22.
-21.
-20.
-19.
-18.
12.
11.
10.
9.
8.
7.
LATITUDE
LONGITUDE

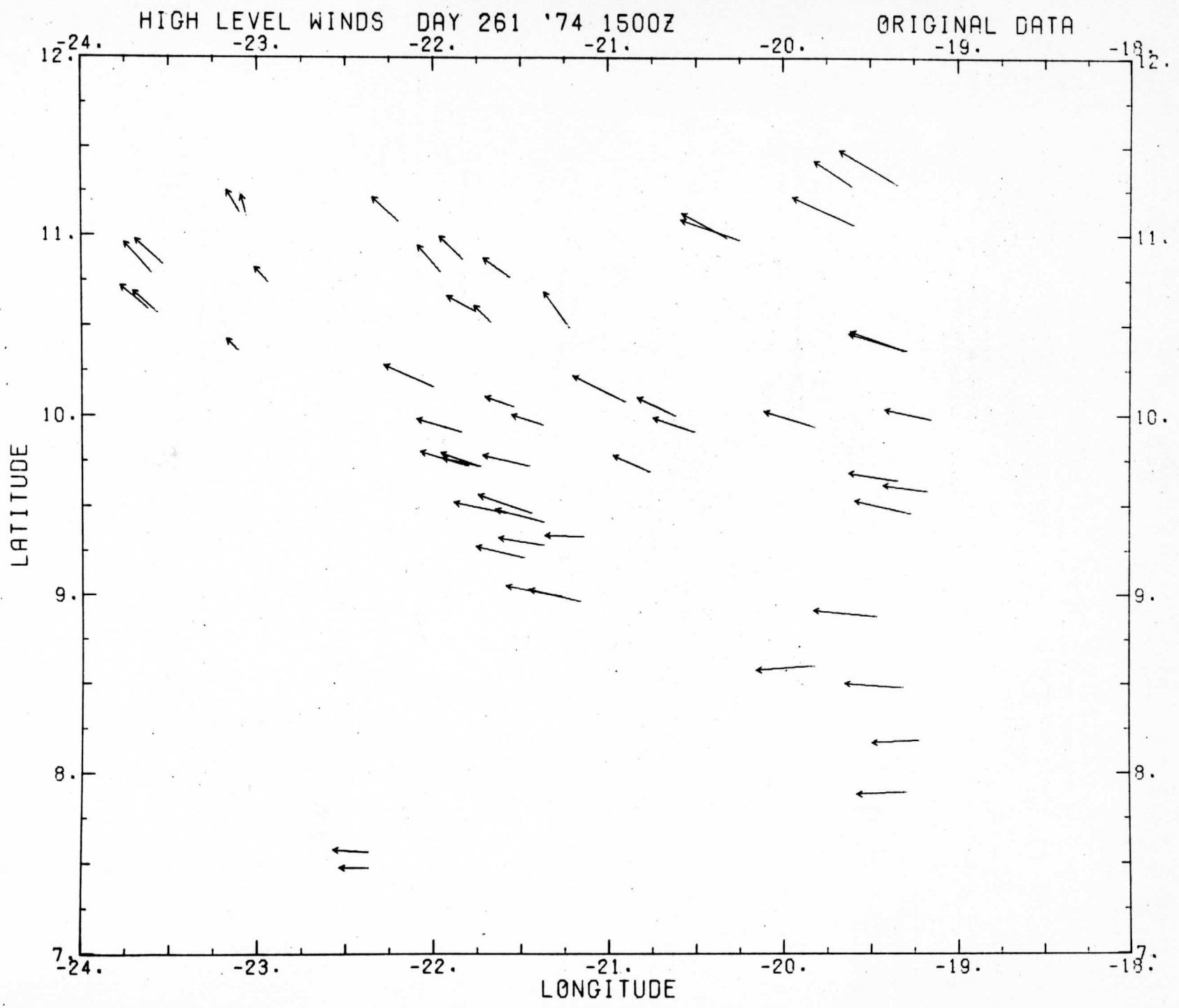
HIGH LEVEL WINDS DAY 261 '74 1500Z
ORIGINAL DATA
-24.
-23.
-22.
-21.
-20.
-19.
-18.
12.
11.
10.
9.
8.
7.
LATITUDE
LONGITUDE